Ex-vivo systems for neuromodulation

A comparison of ex-vivo and in-vivo large animal nerve electrophysiology

Ribeiro, Mafalda; Andreis, Felipe R; Jabban, Leen; Nielsen, Thomas Gomes Nørgaard dos Santos; Smirnov, Sergey V; Lutteroth, Christof; Proulx, Michael J; Rocha, Paulo R F; Metcalfe, Benjamin

Published in:
Journal of Neuroscience Methods

DOI (link to publication from Publisher):
10.1016/j.jneumeth.2024.110116

Publication date:
2024

Document Version
Publisher's PDF, also known as Version of record

Journal of Neuroscience Methods 406 (2024) 110116

Contents lists available at ScienceDirect

Journal of Neuroscience Methods

journal homepage: www.elsevier.com/locate/jneumeth

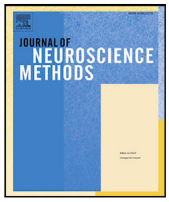

Ex-vivo systems for neuromodulation: A comparison of ex-vivo and in-vivo large animal nerve electrophysiology

Mafalda Ribeiro [a,b], Felipe R. Andreis [c], Leen Jabban [b], Thomas G.N.dS. Nielsen [c], Sergey V. Smirnov [d], Christof Lutteroth [a,e], Michael J. Proulx [a,f], Paulo R.F. Rocha [g], Benjamin Metcalfe [a,h,*]

[a] Centre for Accountable, Responsible, and Transparent AI (ART-AI), Department of Computer Science, University of Bath, Claverton Down, Bath, BA2 7AY, United Kingdom
[b] Department of Electronic & Electrical Engineering, University of Bath, Claverton Down, Bath, BA2 7AY, United Kingdom
[c] Centre for Neuroplasticity and Pain (CNAP), Department of Health Science and Technology, Aalborg University, Selma Lagerløfs Vej 249, 9260, Gistrup, Denmark
[d] Department of Life Sciences, University of Bath, Claverton Down, Bath, BA2 7AY, United Kingdom
[e] Department of Computer Science, University of Bath, Claverton Down, Bath, BA2 7AY, United Kingdom
[f] Department of Psychology, University of Bath, Claverton Down, Bath, BA2 7AY, United Kingdom
[g] Centre for Functional Ecology - Science for People & the Planet (CFE), TERRA Associate Laboratory, Department of Life Sciences, University of Coimbra, Calçada Martim de Freitas, 3000-456, Coimbra, Portugal
[h] The Bath Institute for the Augmented Human, University of Bath, Claverton Down, Bath, BA2 7AY, United Kingdom

ARTICLE INFO

Keywords:
Neuromodulation
Ex-vivo
Peripheral nerves
Multi-electrode cuffs

ABSTRACT

Background Little research exists on extending ex-vivo systems to large animal nerves, and to the best of our knowledge, there has yet to be a study comparing these against in-vivo data. This paper details the first ex-vivo system for large animal peripheral nerves to be compared with in-vivo results.

New Method Detailed ex-vivo and in-vivo closed-loop neuromodulation experiments were conducted on pig ulnar nerves. Temperatures from 20 °C to 37 °C were evaluated for the ex-vivo system. The data were analysed in the time and velocity domains, and a regression analysis established how evoked compound action potential amplitude and modal conduction velocity (CV) varied with temperature and time after explantation.

Main results Pig ulnar nerves were sustained ex-vivo up to 5 h post-explantation. CV distributions of ex-vivo and in-vivo data were compared, showing closer correspondence at 37 °C. Regression analysis results also demonstrated that modal CV and time since explantation were negatively correlated, whereas modal CV and temperature were positively correlated.

Comparison with Existing Methods Previous ex-vivo systems were primarily aimed at small animal nerves, and we are not aware of an ex-vivo system to be directly compared with in-vivo data. This new approach provides a route to understand how ex-vivo systems for large animal nerves can be developed and compared with in-vivo data.

Conclusion The proposed ex-vivo system results were compared with those seen in-vivo, providing new insights into large animal nerve activity post-explantation. Such a system is crucial for complementing in-vivo experiments, maximising collected experimental data, and accelerating neural interface development.

1. Introduction

Electrical stimulation of the nervous system is becoming increasingly prevalent in diagnostic and therapeutic contexts. In recent years, stimulation of the central and peripheral nervous systems (CNS and PNS) has been used for a growing list of indications, such as drug-resistant epilepsy, depression, and spinal cord injury (Creasey et al., 2004; Cracchiolo et al., 2021; Pérez-Carbonell et al., 2020; Bottomley et al., 2020). Neuromodulation of ulnar nerve activity, in particular, has gathered significant research interest in recent years, given the ease of electrode implantation and the range of conditions that can be addressed. Specifically, given that the ulnar nerve extends into the forearm and hand, it is an ideal target for treating peripheral nerve

* Corresponding author at: The Bath Institute for the Augmented Human, University of Bath, Claverton Down, Bath, BA2 7AY, United Kingdom.
E-mail addresses: mr611@bath.ac.uk (M. Ribeiro), b.w.metcalfe@bath.ac.uk (B. Metcalfe).

https://doi.org/10.1016/j.jneumeth.2024.110116
Received 6 November 2023; Received in revised form 5 March 2024; Accepted 21 March 2024
Available online 26 March 2024

injuries, restoring sensory feedback, and restoring motor control. The ulnar nerve can also be examined to treat neuromuscular disorders, such as polyneuropathy and carpal tunnel syndrome (Tan et al., 2015; Fuglsang-Frederiksen and Pugdahl, 2011).

However, current commercially available neurostimulators rely on open-loop stimulation, where a physician manually modifies stimulation parameters to improve efficacy or minimise side effects. Using the example of drug-resistant epilepsy, which affects up to 30% of patients with epilepsy, it is possible to stimulate either the brain with deep brain stimulation (DBS) or the vagus nerve with vagus nerve stimulation (VNS) to minimise seizure frequency. VNS is a particularly appealing solution since it is less invasive than DBS and still effective, reducing seizure frequency by up to 50% in 26%–40% of patients in one year (Pérez-Carbonell et al., 2020). However, since the vagus nerve innervates various organs, side-effects from VNS may arise, including hoarseness, voice alteration, and dyspnoea, due to off-target modulation of nearby muscle or nerve fibres in the neck (Nicolai et al., 2020; Ferrari et al., 2017; Kuba et al., 2009). Moving towards a closed-loop approach, where stimulation parameters are automatically adjusted based on recorded physiological and bioelectronic signal changes, increases stimulation efficacy, improves the clinical benefit, and reduces side effects from stimulation more rapidly (Sun and Morrell, 2014). In the past decade, algorithms ranging from simple filtering and thresholds to machine learning (ML) have been used to denoise, process, and decode neural activity (Shin et al., 2022; Ribeiro et al., 2023). ML, in particular, has shown to be more accurate in detecting symptoms for various neurological conditions and improving the accuracy of motor intention decoding in brain–machine interfaces (BMIs), and hence, has gathered significant interest for closing the loop in neural interfaces for the CNS and PNS.

The gold standard for developing pre-clinical closed-loop neural interfaces is in-vivo animal experiments, and that for verifying their efficacy and safety in patients is human trials. However, relying solely on in-vivo experiments to develop novel neural implants is not conducive to rapidly trialling, optimising, and maximising data capture for these interfaces, given the cost, duration, and ethical issues associated with such experiments. During acute in-vivo experiments, typically only a single nerve will be examined, and the animal will be terminated at the end of the experiment. Given the potential interactions when conducting experiments on multiple sites, examining multiple nerves simultaneously in specific in-vivo experiments can be impractical or unsuitable.

A range of ex-vivo systems have been previously proposed for examining various nerves, namely optic, sciatic, subdiaphragmatic, median, and spinal rootlets (Bastian et al., 2020; Li and Shi, 2006; Tarotin et al., 2022; Harreby et al., 2013; Gribi et al., 2018). These studies typically maximise nerve viability by incorporating isotonic solutions, such as Krebs solution or Ringer's buffer, which can be oxygenated and perfused through one or more chambers at a temperature of 37 to 38 °C to match in-vivo conditions. Sun et al. (2020) describe one of these systems in detail, as well as additional steps of cooling explanted rodent sciatic nerves for an hour in a container with HEPES solution prior to transferring to a room-temperature ex-vivo system. The container was surrounded with ice to keep explanted nerves at a temperature ranging from 0.5 to 2.1 °C. Such ex-vivo systems have been used for accurate and cost-effective experimentation on cells and tissues, and hence maximise experimental data collected from animals. These systems support initiatives such as the 3Rs (Replacement, Reduction, and Refinement) in the United Kingdom that highlight the need for optimising and reducing the number of animals used in in-vivo experiments (Prescott and Lidster, 2017). However, ex-vivo systems are less suitable for investigating whole system physiology, for example, in motor control tasks. Although ex-vivo systems for explanted animal nerves do not fully eliminate ethical concerns, they would maximise the amount of data and information collected on a particular nerve in cases where animal studies cannot be avoided. In the long term, an established ex-vivo neuromodulation system can use explants from animals used for other purposes, hence reducing animal numbers for experimentation. As far as we know, there has also yet to be a study that directly compares ex-vivo large animal nerve activity with that seen in-vivo, and how this changes over time in an ex-vivo system, particularly after transporting explanted nerves (Ribeiro et al., 2022). Large animals, such as pigs and sheep, are not as well-characterised as small animals, such as rodents and rabbits, and require more complex surgical processes, but the gross anatomy, approaches, equipment, and electrodes used have the potential to be directly translated to humans (Koh et al., 2022).

Therefore, we aimed to develop an ex-vivo neuromodulation system for large animal nerves, and establish how results in this system compare with those seen in-vivo. Both ex-vivo and in-vivo neuromodulation experiments were carried out, for which recordings of evoked compound action potentials (eCAPs) were then analysed both in the time and the velocity domains and at different temperatures in the ex-vivo case. Finally, a regression analysis was conducted for the ex-vivo data to investigate the correlation between eCAP features, such as amplitude and conduction velocity (CV), and experimental parameters, such as temperature and the time since explanting the nerve, to assess nerve function and viability. These findings are crucial for increasing confidence in, and hence promoting the adoption of ex-vivo systems more broadly to accelerate neuromodulation research using large animal models.

2. Methods

2.1. Experimental protocol

A schematic of the experimental set-up and the in-vivo and ex-vivo protocols is shown in Fig. 1 and described here. Recording and stimulation multi-electrode cuffs (MECs) were manufactured and implanted in-vivo on the pig ulnar nerve. A charge-balanced, biphasic stimulation profile was applied, covering stimulation currents up to 16 mA, and the resulting eCAPs were recorded. This stimulation protocol was repeated four times per recording. The nerve was subsequently explanted, transported over the course of an hour in Ringer's buffer at 4 °C, and transferred to the ex-vivo system containing the same solution. The temperature of the ex-vivo system was initially 20 °C, and was then gradually increased to a maximum of 37 °C using a temperature-controlled water bath, which in turn supplied a water jacket surrounding the Ringer's buffer containing the nerve. During this time, the same stimulation protocol as that used in-vivo was applied. Both in-vivo and ex-vivo datasets were processed and examined in the time and velocity domains. Lastly, a regression analysis was also conducted with the ex-vivo data to ascertain the impact of key parameters, such as time since explanting the nerve and temperature, on the eCAP amplitude and modal CV.

2.2. Cuff design

Stimulation and recording cuffs were manufactured and implanted on the ulnar nerve first in-vivo, then ex-vivo. The cuffs were manufactured using the technique described by Haugland (1996). The stimulation cuff was manufactured with a tripolar configuration, with three platinum-iridium ring electrodes with 3 mm centre-to-centre distance and a total cuff length of 10 mm. The outer electrodes in the stimulation cuff had a width of 1 mm and the inner electrode a width of 0.5 mm. The recording cuff consisted of 12 platinum-iridium ring electrodes and an additional two guard electrodes of the same material on either end, which were short-circuited and used as a reference. The recording cuff had a total length of 50 mm, an inter-electrode distance of 3.5 mm, the recording electrodes had a width of 0.5 mm, and the guard electrodes had a width of 1 mm. The inner diameter for the stimulation and recording cuffs were 1.8 mm and 2.6 mm, respectively.

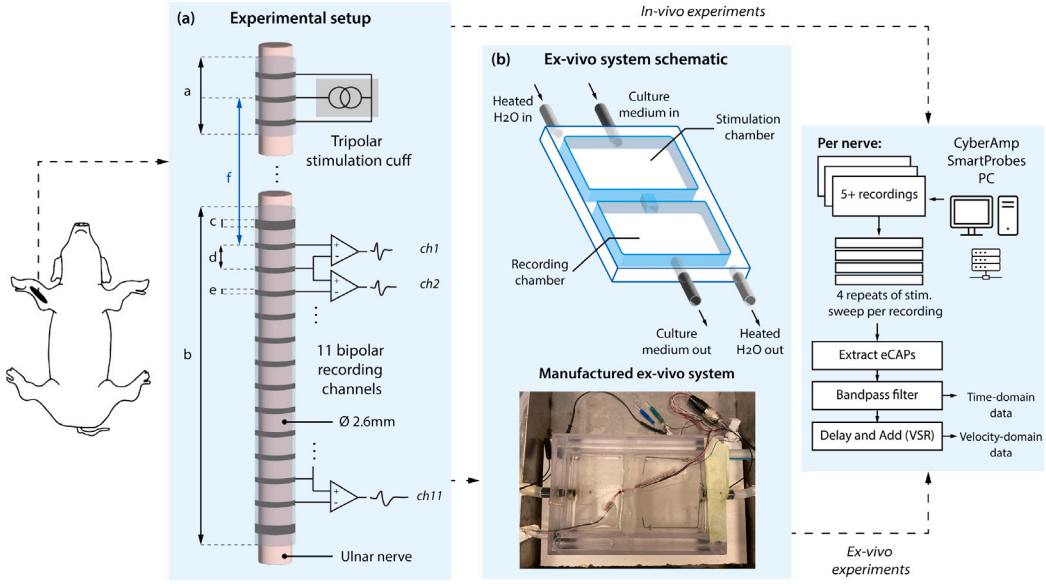

Fig. 1. Experimental setup for in-vivo and ex-vivo experiments. (a) Diagram of stimulation and recording cuffs. The length of the tripolar stimulation cuff, *a*, is 10 mm. The recording multi-electrode cuff (MEC) consisted of 11 channels (labelled *ch*1 to *ch*11) spread over an overall length, *b*, of 50 mm. The width of each recording electrode, *e*, was 0.5 mm, and the inter-electrode distance, *d*, was 3.5 mm. Guard electrodes were also included at the start and end of the recording MEC, with a width, *c*, of 1 mm, and short-circuited to create a reference. A distance *f* has also been labelled, corresponding to the distance between the first recording electrode and the middle of the stimulation cuff. In the ex-vivo system, *f* ranged from 32 to 55 mm. (b) Schematic diagram (above) showing two chambers and pathways for heated water and chamber perfusion. Image of the manufactured ex-vivo system (below). The recording and stimulation cuffs were placed in separate chambers, joined by a narrow channel in the middle of the ex-vivo system.

Different cuff diameters were selected for stimulation and recording given that in-vivo, the nerve diameter is slightly smaller distally (where the stimulation cuff was implanted) compared to more proximally (where the recording cuff was implanted). In a prior histology study on pig ulnar nerves, the proximal main trunk was found to have a mean diameter of 1.71 mm, and the distal end of the ulnar nerve had a mean diameter of 1.30 mm (Andreis et al., 2024). Fig. 1(a) shows a schematic representation of the neural interfaces used in this study.

2.3. Surgical methods

All animal procedures were performed in accordance with the *Danish Animal Experiments Inspectorate* (ethics approval number 2017-15-0201-01317), as well as the care and use of laboratory animals as described by the *U.S. National Institutes of Health*. Four Landrace pigs with weights ranging between 32.4 and 34.8 kg were used for the study described in this paper. The pigs were anaesthetised with an intramuscular injection of ZoletilVet (1.5 mg/10 kg; a mixture of ketamine 8.3 mg mL^{-1}, tiletamine 8.3 mg mL^{-1}, zolazepam 8.3 mg mL^{-1}, butorphanol 1.7 mg mL^{-1}, xylazine 8.3 mg mL^{-1}). The animals were then kept sedated using sevoflurane (1.5 to 2.5% minimum alveolar concentration), propofol (2 mg h^{-1} kg^{-1}) and fentanyl (10 µg h^{-1} kg^{-1}), administered intravenously. The animals were mechanically ventilated at a rate of 15 cycles per minute. Throughout all experiments, the body temperature, near-nerve temperature, end-tidal CO_2, oxygen saturation, heart rate, respiratory rate, blood pressure, and tail reflex were monitored. The mean near-nerve temperature was 38 °C and ranged between 37.8 and 38.3 °C.

For each pig, a 20 cm incision was made to expose the ulnar nerve through the anterior forelimb, which was subsequently dissected as far distally as permissible. A section of approximately 15 cm was freed, the recording cuff was implanted at the most proximal aspect of the ulnar nerve, and the stimulation cuff was implanted distally (proximal to the elbow). A silicone sheet was applied around the cuffs to minimise current leakage, and sutures were added to each end and the centre of the recording cuff to ensure these were closed and in good contact with the nerve. Upon completing in-vivo recordings, the animal was euthanised by an overdose of pentobarbitone administered intravenously, the cuffs were explanted, and subsequently, the nerve was explanted and stored in a closed container with Ringer's solution at 4 °C. The proximal nerve end was tagged with a suture to help replicate the original stimulation and recording cuff orientations ex-vivo. The nerve was then transported to the ex-vivo system over the course of one hour, following a realistic use case where transportation between the operating theatre and a separate electrophysiology lab is required. Ex-vivo recordings started between 2 and 3 h after explanting the nerve, including the transport time of one hour.

2.4. Ex-vivo system

An ex-vivo system was designed and manufactured to sustain explanted animal nerves with lengths in the order of several centimetres in modified Ringer's buffer. The main container, depicted in Fig. 1(b), was made of acrylic and consisted of two chambers joined by a narrow channel at the centre. A temperature-controlled water bath connected to a water jacket surrounding the chambers was also used to maintain the nerve medium at a set temperature. Supplementary oxygen was not provided to the nerve medium. The nerve was submersed in modified HEPES-containing Ringer's buffer with (in mmol L^{-1}) 146 NaCl, 5 KCl, 1 $MgCl_2$, 2 $CaCl_2$, 10 HEPES, 11 glucose, pH adjusted to 7.4 using NaOH. This medium was selected given it was previously shown to promote the viability of explanted nerves (Harreby et al., 2013).

Both chambers were filled with modified Ringer's buffer at 20 °C to allow the nerve to warm up gradually once submerged. The nerve was threaded through the channel, and the stimulation and recording cuffs were applied to the ends of the nerve in different chambers to minimise the impact of stimulation artefacts on the recordings. The distance between the middle of the tripolar stimulation cuff and the first recording electrode in ex-vivo experiments (labelled as *f* in Fig. 1(a)) ranged from 32 to 55 mm. The temperature protocol was to collect recordings at a range of temperatures between the initial (minimum) temperature of 20 °C and a maximum of 37 °C. The nerve was kept at each temperature for a minimum of 10 min. In practice, temperature control was challenging, and it took significant time (often >20 min) for the system loop temperature to stabilise. As a result, although the same stimulation patterns were applied with an equal

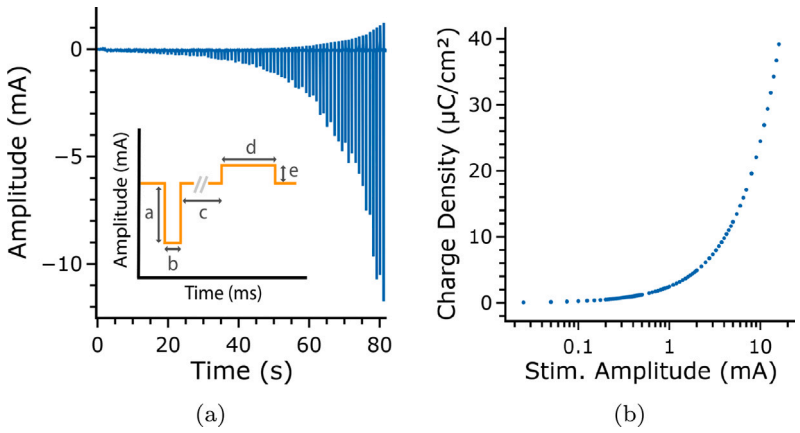

Fig. 2. Overview of stimulation profile delivered to the nerve both ex-vivo and in-vivo. (a) Amplitude plot of sweep of stimulation pulses, repeated four times in each individual recording. Inset: Diagrammatic representation of single biphasic stimulation pulse, where a is the cathodic pulse amplitude (0–16 mA), b is the cathodic pulse width (100 μs), c is the interphase interval (32 ms), d is the anodic pulse width (1 ms), and e is the anodic stimulation amplitude (10% of cathodic pulse amplitude). (b) Quantified charge density for each stimulation level (based on cathodic pulse only).

number of repeats to all nerves, the temperature increments between 20 °C and 37 °C were not consistent between animals. For Pig 1 there were four increments, for Pig 2 seven, and for Pig 3 six. For one of the explanted nerves, the recorded eCAP amplitude was below a threshold of ~3σ above the baseline at 30 °C. In this case, to maintain nerve viability, the maximum temperature attained was 30 °C, and after this peak, an additional ten recordings were carried out as the nerve cooled to a minimum temperature of 26 °C. Nerve viability was assessed by the ability to recruit eCAPs, which was accomplished for up to 5 h post-explantation in this study.

2.5. Electronic apparatus

A biphasic stimulation waveform was delivered to the nerve both ex-vivo and in-vivo to elicit eCAPs. This was achieved using a programmable current stimulator (STG4008, Multichannel Systems) set up to deliver charge-balanced pulses, with the primary cathodic phase increasing from an amplitude of 0 to 16 mA (beyond supramaximal level). The cathodic phase lasted 100 μs and was followed by a 32 ms pause, prior to delivering an anodic phase lasting 1 ms at an amplitude of 10% the cathodic amplitude. The longer duration and lower amplitude of the anodic phase were chosen to allow for the recovery of charge from the electrode without suppressing or counteracting the stimulation effect of the cathodic phase. The maximum charge density was, therefore, 39.2 μC cm^{-2}. The long interphase delay was chosen to investigate secondary pulse excitability, but these results are not presented here. Each biphasic pulse was separated by a 1 s delay. The stimulation amplitude was increased in a step size of 50 μA at lower stimulation amplitudes to have a fine grain view of nerve recruitment, but beyond the 7 mA mark (supramaximal level) this was increased to 1 mA increments. The entire stimulation profile was repeated four times per recording, hence the total duration of stimulation was 5 min per recording. The entire stimulation profile is shown in Fig. 2(a), with an inset showing a diagram of a single biphasic pulse, and the quantified charge density for the cathodic pulse at each stimulation amplitude is shown in Fig. 2(b).

The 11 recording channels of the recording cuff were connected to ultra-low noise differential amplifiers (AI402 SmartProbes, Axon Instruments, Inc.) and a programmable signal conditioner (CyberAmp 380, Axons Instruments, Inc.) in a bipolar configuration. The total amplifier gain ranged between 5000× and 100,000×, and the data was band-pass filtered with a fourth-order Bessel filter with cutoff frequencies of 100 Hz and 10 kHz. All data were digitised using a PCIe-6363 card (National Instruments), with each channel being sampled at 90 kHz with 16-bit resolution.

2.6. Data analysis

All data processing and analyses were conducted offline using Python and R. After digitisation, the data were band-pass filtered with a fifth-order Butterworth filter with cutoff frequencies of 100 Hz and 5 kHz, and eCAPs were extracted and analysed in the time and the velocity domains. Prior studies on the pig ulnar nerve have shown eCAP duration to be between 1 and 2 ms when the distance between the stimulating and first recording electrodes was around 25 mm, which is similar to the distances in this study (Andreis et al., 2022a,b). With an expected CV range from 10 to 100 m s^{-1} and a recording cuff length of 50 mm, it is expected that fibre action potentials (APs) would take between 0.5 and 5 ms to propagate through all recording channels. Hence, for the time-domain analysis in this work, windows of 10 ms after each stimulus containing eCAPs were extracted for every channel, stimulation level, and temperature. For the velocity-domain analysis, a *delay-and-add* beamforming algorithm based on velocity-selective recording (VSR) (Taylor et al., 2012; Metcalfe et al., 2021) was applied to the windows of data to produce an intrinsic velocity spectrum (IVS). This approach follows the logic that for a MEC with equally separated ring electrodes, the delay between each recorded CAP arises owing to the contributing fibre CVs and inter-electrode spacing. Therefore, a delay τ can be calculated for each channel to effectively cancel the naturally occurring delay. This delay can be swept through a range of values, and when summing the different channel data, the output peaks at d/v, where d is the inter-electrode spacing and v is the CV of the CAP. This technique, therefore, increases the effective SNR by $\sqrt{C}$, where C is the number of channels, and minimises common-mode interference.

In total, four pig ulnar nerves were examined for this work. Both in-vivo and ex-vivo data were collected for two of these nerves, making these results directly comparable. One ex-vivo and one in-vivo dataset were collected from two additional but different nerves. In summary, there were three sets of data of each type, ex-vivo and in-vivo, but only two sets were directly comparable since they originated from the same nerve. Furthermore, as mentioned in Section 2.4, two nerves were heated up to a maximum temperature of 37 °C, whereas one nerve was only heated up to 30 °C given eCAP amplitude started to decrease at this temperature point.

2.7. Regression analysis

It is unclear how the viability of explanted, large animal nerves progresses in an ex-vivo system, particularly if these must be transported between laboratories. In the context of this work, nerve viability is assumed to be continuous and hence dependent on the number of

individual fibres that are still active, rather than a binary measure where the nerve is either entirely viable or not at all. Prior studies have examined nerve fibre CV following temperature alterations (Waxman, 1980; Johnson and Olsen, 1960) and showed that CV decreases with decreasing temperatures. However, to the best of our knowledge, the relationship between modal CV and temperature has yet to be characterised for peripheral nerves ex-vivo. Similarly, nerve health and viability have yet to be examined in a spontaneous manner, particularly under sub-optimal oxygen and nutrient supply, as would be the case in the ex-vivo system described in this work. Bearing in mind results from prior in-vivo studies (Waxman, 1980; Johnson and Olsen, 1960), it is hypothesised that for the ex-vivo experiments carried out in this study:

- **H1** The modal eCAP CV will decrease with time elapsed since explanting the nerve.
- **H2** As temperature increases in the ex-vivo system, so will the modal CV.
- **H3** As temperature increases up to 37 °C without supplementary oxygen in the ex-vivo system, all fibres will degrade faster, which will present a decrease in eCAP amplitude.
- **H4** As temperature increases up to 37 °C, the modal eCAP CV will approach that seen in-vivo.

Given that the time since explanting the nerve and temperature can affect nerve eCAP amplitude and CV, a regression analysis was carried out to test the hypotheses above, describe any observed trends, and understand the individual contribution of these two key variables. Therefore, the ex-vivo data were further processed and collated with relevant experimental variables to aid in investigating the hypotheses proposed above. In short, the following dependent variables were extracted for each individual eCAP recording:

1. Peak-to-peak eCAP amplitude in μV
2. Modal velocity from the IVS in $\mathrm{m\,s^{-1}}$

And the following independent variables were also collected at the time of each eCAP recording:

1. Stimulation current in mA
2. Time since explanting the nerve in min
3. Temperature of the Ringer's medium in the ex-vivo system in °C
4. Distance between the first recording electrode and stimulation site in mm, measured from the centre of the first recording electrode to the centre of the middle contact of the tripolar stimulation cuff (see Fig. 1(a))

As a starting point, all ex-vivo data at all stimulation levels were loaded, and eCAPs were included if they were clearly visible in the recording. This was achieved in practice by checking if there was a minimum of 20 consecutive samples above the channel mean plus 2 standard deviations (σ) of the channel data. Following this check, peak height calculations were carried out, both in the time and the velocity domains to extract the peak-to-peak eCAP amplitude and modal CV from the IVS. The width of each eCAP in the time domain was also calculated using standard peak width finding functions, using a relative peak height of 0.3. The corresponding time since explantation and temperature were collated with this information. In total, three separate pig nerves were analysed (all the ex-vivo data available), with a total of 27 recordings collected and a minimum of 4 recordings per nerve.

Using the features listed above, two multivariate generalised least squares (GLS) linear regression models were fit in R using the *nlme* package (Bliese, 2022). Two response variables, the eCAP amplitude and the modal eCAP CV, were investigated separately in the two models. A compound symmetry correlation structure was used with a grouping factor of experiment and recording number. The regression coefficients were tested for significance with $\alpha = .05$, reporting 95% confidence intervals (CI). The independent variables listed above were used for both regression models. The channel number had a visible impact on eCAP amplitude, so this was included as an independent variable in the eCAP amplitude model. However, given that all channels were used for calculating the modal eCAP CV using VSR, the channel number as an independent variable was excluded in this model.

3. Results

3.1. Time-domain analysis

3.1.1. Evoked response at varying stimulation amplitudes

Fig. 3(a) and (b) show the increase in eCAP amplitude both ex-vivo and in-vivo for the same nerve with increasing stimulation amplitude up to a maximum level of 16 mA. As the stimulation current increases, a greater number of APs are elicited, increasing the amplitude of the eCAP. For Fig. 3(a) and subsequent figures showing example ex-vivo data at 37 °C, the time since explantation was 5 h, and the distance between the stimulation and first recording sites was 32 mm. Recorded eCAPs both ex-vivo and in-vivo were plotted and analysed in the time domain at 37 to 38 °C. Fig. 3(c) and (d) highlight the mean eCAP morphology seen in-vivo and ex-vivo at a supramaximal stimulation current of 16 mA with min–max normalisation and detrending.

Visible eCAPs were extracted from recordings by finding at least 20 consecutive samples (approx. 0.2 ms) 2σ above each channel mean, to account for varying baseline noise levels. Table 1 shows numerical results for these amplitude and width calculations, from the same recording channel at supramaximal stimulation currents (>5 mA). For ex-vivo recordings, the eCAP amplitude was 83 ± 51 μVpp (peak-to-peak), whereas the in-vivo amplitude was 170 ± 110 μVpp. At these stimulation currents, ex-vivo eCAPs had an average duration of 0.04 ± 0.02 ms whereas in-vivo eCAPs had an average duration of 0.17 ± 0.05 ms. Ex-vivo results at 20 °C have also been included in Table 1, showing an increase in eCAP width at lower temperatures. Table 2 shows these measurements for each individual animal nerve, where the data for Pig 1 corresponds to the example plots in Fig. 3(a) and (b). The discrepancy seen here in eCAP amplitude can be potentially explained by changes in the tissue-electrode interface after explanting the nerve and re-implanting both the simulation and recording cuffs. This difference can also be explained in part owing to the recording cuff being implanted proximally and the stimulation cuff being implanted distally (proximal to the elbow) for in-vivo experiments, which implies a larger propagation distance for in-vivo eCAPs and, hence, increased dispersion of the individual APs (see Discussion).

3.1.2. Evoked response at increasing temperature (up to 37 °C)

When transferring the explanted nerve to the ex-vivo preparation, the temperature was gradually increased from 20 °C to 37 °C. Fig. 4(a) shows an example of the changes in eCAP morphology as temperature increases, namely that the duration of the eCAP decreases from 0.1 to 0.07 ms and the amplitude increases up to ~300 μVpp at 32 °C, before decreasing to ~230 μVpp at 37 °C. For Fig. 4(a) and subsequent figures showing examples of ex-vivo data at this range of temperatures, the time since explantation was 4 to 5 h, and the distance between the stimulation and first recording sites was 32 mm. The eCAP seen ex-vivo at 37 °C was also compared to that for the same nerve in-vivo, as shown in Fig. 4(b). A good agreement can be seen between both eCAP shapes.

To further quantify the differences in fibre recruitment between ex-vivo and in-vivo recordings, recruitment curves (Andreis et al., 2022b) were also obtained to compare the peak eCAP amplitude at each stimulation current for different temperatures ex-vivo and on average ex-vivo and in-vivo. Fig. 5(a) highlights the changes in the recruitment curves when increasing the temperature ex-vivo for one example experiment, which highlights a shift in the threshold for supramaximal activity when increasing the temperature from 20 to 37 °C, with the threshold being decreasing from 1 mA to 500 μA. The changes in eCAP amplitude previously seen in Fig. 4(a) can also be seen here. Fig. 5(b) shows the

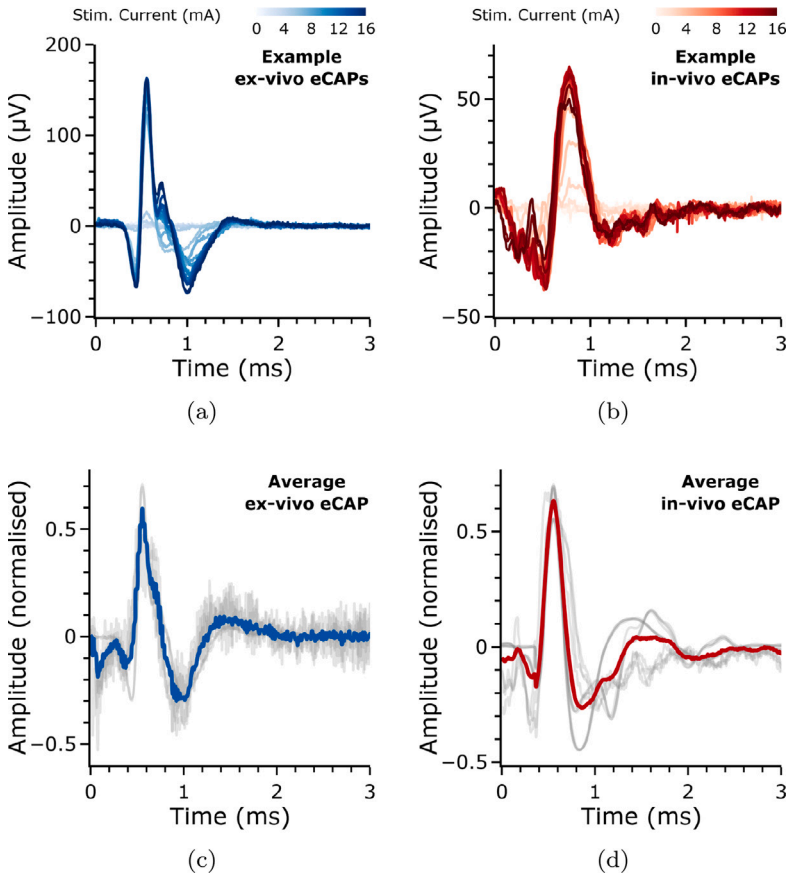

Fig. 3. Overview of eCAP morphology as at stimulation currents ranging between 0 and 16 mA, as well as at supramaximal stimulation ex-vivo and in-vivo at 37 to 38 °C. (a) Single channel plot of example ex-vivo eCAPs across the entire stimulation amplitude sweep. (b) Single channel plot of in-vivo eCAPs across the entire stimulation amplitude sweep for the same nerve as (a). (c) Average ex-vivo (blue) responses at a supramaximal stimulation level of 16 mA. (data from 2 nerves). (d) Average in-vivo (red) responses at a supramaximal stimulation level of 16 mA. (data from 3 nerves) (Stimulation occurs at time equally zero in these plots, min–max normalisation was used in (c) and (d), and individual nerve recordings are shown in grey in both).

Table 1
Summary of time-domain eCAP features at 20 °C and 37 °C ex-vivo, and at 38 °C in-vivo.

Parameter	Value at 20 °C ex-vivo (mean ± s.d.)	Value at 37 °C ex-vivo (mean ± s.d.)	Value at 38 °C in-vivo (mean ± s.d.)
Supramaximal eCAP amplitude (μV)	79 ± 82	83 ± 51	170 ± 110
Supramaximal eCAP duration (ms)	0.26 ± 0.08	0.04 ± 0.02	0.17 ± 0.05

Table 2
Summary of time-domain eCAP features for each individual animal nerve across all temperatures ex-vivo, at 20 °C and 37 °C ex-vivo, and at 38 °C in-vivo. Note that for Pig 2 the maximum temperature reached was 30 °C.

Animal	Parameter	Average value across all temps. ex-vivo (mean ± s.d.)	Value at 20 °C ex-vivo (mean ± s.d.)	Value at 37 °C ex-vivo (mean ± s.d.)	Value at 38 °C in-vivo (mean ± s.d.)
Pig 1	Supramaximal eCAP amplitude (μV)	250 ± 87	220 ± 1.5	120 ± 2.2	87 ± 8.3
	Supramaximal eCAP duration (ms)	0.22 ± 0.10	0.28 ± 0.00	0.04 ± 0.00	0.23 ± 0.02
Pig 2	Supramaximal eCAP amplitude (μV)	34 ± 8.8	34 ± 4.5	–	110 ± 15
	Supramaximal eCAP duration (ms)	0.19 ± 0.10	0.25 ± 0.08	–	0.11 ± 0.00
Pig 3	Supramaximal eCAP amplitude (μV)	100 ± 70	30 ± 3.2	6.78 ± 3.27	–
	Supramaximal eCAP duration (ms)	0.16 ± 0.08	0.25 ± 0.12	0.04 ± 0.04	–
Pig 4	Supramaximal eCAP amplitude (μV)	–	–	–	320 ± 15
	Supramaximal eCAP duration (ms)	–	–	–	0.16 ± 0.01

average recruitment ex-vivo and in-vivo across multiple nerves. The average recruitment profile in each case was represented by a logistic curve, fitted using Scipy's curve fitting functionality and the following equation:

$$f(x) = \frac{L}{1 + e^{-k(x-x_0)}} + o \quad (1)$$

where L is the curve's maximum value, k is the steepness of the curve, x_0 is the x value at the sigmoid midpoint, and o is a possible offset.

Results show that in-vivo eCAPs start to be recruited on average at 175 μA and reach a supramaximal level beyond 650 μA. Compared with the ex-vivo data, in-vivo eCAPs show a more rapid increase to supramaximal levels.

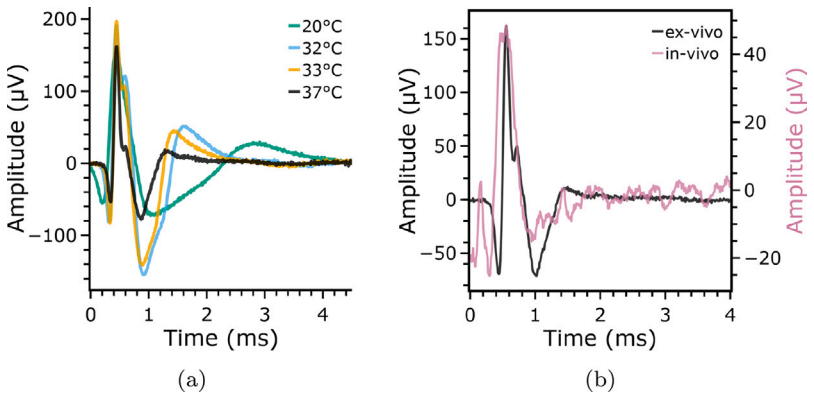

Fig. 4. Example eCAP morphology at temperatures ranging between 20 and 37 °C. (a) Example ex-vivo eCAPs across different temperatures under supramaximal stimulation (16 mA). (b) In-vivo (pink) and ex-vivo (black) responses at 37 to 38 °C under supramaximal stimulation (16 mA) for the same nerve used in (a). In both plots, eCAPs were aligned according to their peaks to provide a more direct comparison of eCAP shape.

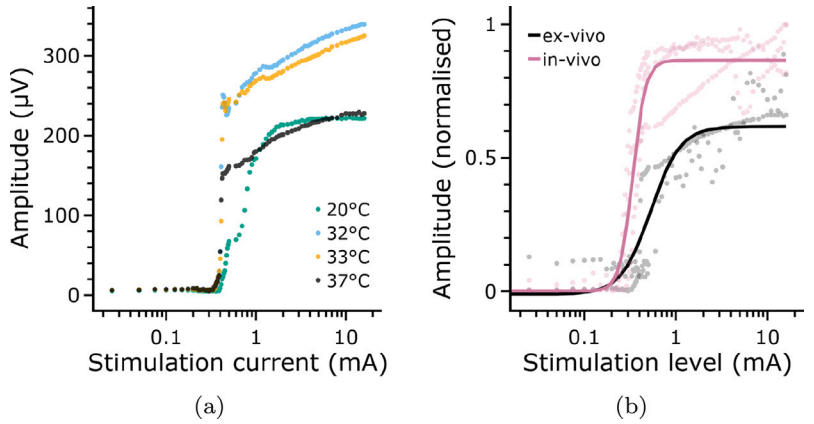

Fig. 5. Recruitment curves for ex-vivo data at temperatures ranging between 20 and 37 °C, and average ex-vivo and in-vivo recruitment curves at 38 °C. In all plots, data points for different recordings are included and displayed as dots. (a) Example ex-vivo experiment at increasing temperatures, from 20 to 37 °C. (b) All ex-vivo and in-vivo experiments at 37 to 38 °C, with min–max normalisation. The solid pink trace represents the average fitted recruitment curve for all in-vivo recordings, whereas the solid black trace represents the average fitted recruitment curve for all ex-vivo recordings.

3.2. Velocity-domain analysis

3.2.1. Recruited velocities at varying stimulation amplitudes

All recordings were also analysed in the velocity domain, and ex-vivo results were compared against those in-vivo. Fig. 6(a) and (b) show example IVS plots throughout the full range of stimulation levels, both ex-vivo and in-vivo. The ex-vivo data shows a narrower modal peak around 45 $m\,s^{-1}$, whereas that for the in-vivo data is wider and centred around 55 $m\,s^{-1}$. Fig. 6(c) shows the average IVS for recordings conducted ex-vivo at 37 °C, highlighting a modal CV of 45 $m\,s^{-1}$, whereas for the in-vivo data shown in Fig. 6(d) the modal CV is at 60 $m\,s^{-1}$. Fig. 6(e) shows the similarity between ex-vivo and in-vivo IVS plots at the same temperature, using shaded areas to show the extent of overlap and the mean-squared error (MSE) between the two. Also included was the MSE when compared with ex-vivo data at a lower temperature of 20 °C, highlighting a 77% reduction in the MSE and hence, improved correspondence between the two when ex-vivo temperatures approach those seen in-vivo.

3.2.2. Recruited velocities at increasing temperature (up to 37 °C)

Given each nerve had to be warmed up to 37 °C in the ex-vivo system, it was also possible to compare the modal CV at each temperature both in the time domain and the velocity domain with multiple IVS plots. Fig. 7(a) shows a straight line fit through each adjacent recording channel to illustrate eCAP propagation along the MEC in the time domain. Approximate modal CV values of 16.7 $m\,s^{-1}$ at 20 °C and 37.7 $m\,s^{-1}$ at 37 °C were obtained following a simple calculation using the distance between electrode sites divided by the onset time of the eCAP at each point, averaged across each channel. A more comprehensive view of the eCAP CV distribution can be obtained using IVS plots, as shown in Fig. 7(b) and (c). Fig. 7(b) demonstrates the contribution of different eCAP velocities at increasing temperatures. This plot shows that as temperature increases, so does the modal eCAP CV, therefore resulting in a shift to the right in the IVS plot. As temperature increases to 32 °C, 33 °C, and finally, 37 °C, the modal CV in the IVS plots also increases to 24, 27, and 43.5 $m\,s^{-1}$, respectively. Fig. 7(c) shows a comparison of the same nerve ex-vivo and in-vivo at 37 to 38 °C, where the modal eCAP CV is 43.5 $m\,s^{-1}$ ex-vivo and 60 $m\,s^{-1}$ in-vivo. A similar plot to that in Fig. 6(c) was produced, highlighting the close overlap between IVS ex-vivo and in-vivo, also quantified by a decrease of 80% in MSE when compared to data at 20 °C.

3.3. Regression analysis

As previously described, two linear regression models were devised to investigate the impact of ex-vivo experimental parameters on eCAP amplitude and the modal CV, respectively. Two independent variables of interest were the time since explanting the nerve and temperature. Table 3 shows the results for the linear regression model for eCAP amplitude. Observationally, the eCAP amplitude is negatively correlated with time since explantation (−0.049 $\mu V\,min^{-1}$, p = 0.7199), and temperature is also negatively correlated (−0.76 $\mu V\,°C^{-1}$, p = 0.7533), but these results are not significant. However, when examining relevant experimental parameters with the modal eCAP CV model instead,

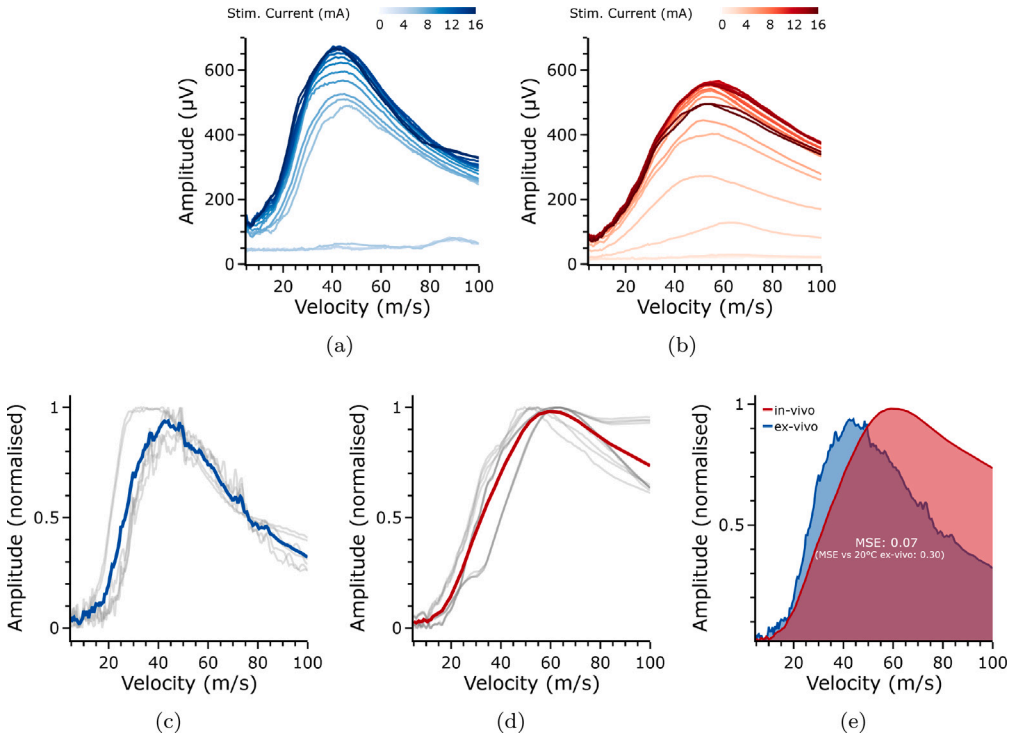

Fig. 6. Intrinsic velocity spectra (IVS) at varying stimulation amplitudes, ranging between 0 and 16 mA, and averaged across ex-vivo and in-vivo data at 37 to 38 °C. (a) Ex-vivo IVS for a single experiment at 37 °C across the entire range of stimulation currents (up to 16 mA). (b) In-vivo IVS for a single experiment across the entire range of stimulation currents (up to 16 mA, same nerve as that for data shown in (a)). (c) Average ex-vivo IVS under supramaximal stimulation at 37 °C (blue line) and individual repeats (grey lines, data from 2 nerves). (d) Average in-vivo IVS under supramaximal stimulation (red line) and individual repeats (grey lines, data from 3 nerves). (e) Comparison of average ex-vivo and in-vivo IVS at 37 to 38 °C in terms of IVS overlap with ex-vivo data in blue and in-vivo data in red and quantified mean-squared error (MSE). MSE was 0.30 vs. ex-vivo IVS at 20 °C, 0.07 vs. ex-vivo IVS at 37 °C.

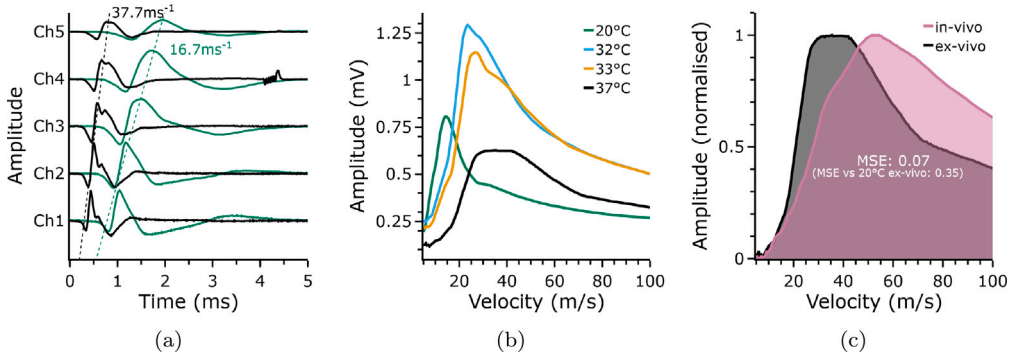

Fig. 7. Recruited velocities at temperatures ranging between 20 and 37 °C from example ex-vivo experiment. (a) Time-domain plot of propagating ex-vivo eCAPs at 20 °C (green) and 37 °C (black), showing modal eCAP velocities of 16.7 m s^{-1} and 37.7 m s^{-1}, respectively. (b) Intrinsic velocity spectra (IVS) of the same ex-vivo data across different temperatures. (c) Comparison of in-vivo (pink) and ex-vivo (black) IVS plots with min–max normalisation at 37 to 38 °C for the same nerve, showing extent of overlap and quantified MSE. MSE was 0.35 vs. ex-vivo IVS at 20 °C, 0.07 vs. ex-vivo IVS at 37 °C.

statistically significant correlations with temperature and time since explantation can now be seen (see Table 4). Specifically, the modal eCAP CV decreases by 0.13 m s^{-1} min^{-1} since the nerve has been explanted ($p < 0.001$) and increases by 2.17 m s^{-1} °C^{-1} ($p < 0.001$). This model's β coefficients further emphasise that time since explanting the nerve and temperature are the two strongest contributors to modal CV.

4. Discussion

In-vitro and ex-vivo systems have been crucial in biomedical research for examining cells and tissues in an accurate and cost-effective way. Prior ex-vivo systems have been predominantly aimed at small animal nerves, which have different surgical and experimental constraints compared to large animals (Li and Shi, 2006; Gribi et al., 2018; Bastian et al., 2020). Only a limited number of studies mention ex-vivo preparations for large animal nerves (Harreby et al., 2013; Tarotin et al., 2022), which have greater potential to be directly translated to humans. Additionally, to the best of our knowledge, there has yet to be a study that directly compares ex-vivo large animal nerve activity with that seen in-vivo, and how this changes over time in an ex-vivo system.

Hence, this work describes the development of an ex-vivo system suitable for conducting neuromodulation experiments on large explanted animal peripheral nerves. Electrical activity in this system was also compared with that seen in-vivo, and changes in nerve activity were assessed over time and at different temperatures ex-vivo. This was examined in the context of having to transport explanted ulnar nerves between the operating theatre and a separate laboratory for ex-vivo experiments, which is a realistic use case for large animal studies.

Table 3
Multivariate linear regression results with the *eCAP amplitude* as the dependent variable, where **B** are the model coefficients with raw data and β are model coefficients with z-score normalised data. Statistically significant p-values are shown in bold.

Coefficient	**B** (Δμ V)	β	CI (95%)	Std error	t-value	p-value
Time since explantation (min)	−0.049	−0.059	−0.31–0.22	0.14	−0.36	0.7199
Temperature (°C)	−0.76	−0.047	−5.47–3.96	2.40	−0.31	0.7533
Channel	−4.32	−0.23	−4.48 to −4.15	0.086	−50.09	**<0.001**
Distance to stim. site (mm)	−1.83	−0.36	−4.48 to −4.15	0.74	−2.46	**0.0140**
Stimulation level (mA)	2.30	0.16	2.17–2.43	0.066	34.60	**<0.001**
(Intercept)	171.61	−0.035	26.05–317.16	74.26	2.31	0.0208
R^2	0.29					

Table 4
Multivariate linear regression results with the *modal eCAP CV* as the dependent variable, where **B** are the model coefficients with raw data and β are model coefficients with z-score normalised data. Statistically significant p-values are shown in bold.

Coefficient	**B** ($\Delta m\,s^{-1}$)	β	CI (95%)	Std error	t-value	p-value
Time since explantation (min)	0.13	−0.81	−0.15 to −0.11	0.011	−11.89	**<0.001**
Temperature (°C)	2.17	0.70	1.79–2.54	0.19	11.38	**<0.001**
Distance to stim. site (mm)	−0.10	−0.11	−0.22–0.014	0.059	−1.73	0.0840
Stimulation level (mA)	0.026	0.010	0.0058–0.046	0.010	2.53	**0.0113**
(Intercept)	5.12	0.0046	−6.41–16.62	5.87	0.87	0.3846
R^2	0.70					

Porcine ulnar nerves were used given their resemblance to human anatomy, the ease of implantation, and the range of conditions which can be addressed with neuromodulation on the ulnar nerve (Andreis et al., 2022a).

After cooling the nerves to 4 °C for transportation and reheating them back to between 20 and 37 °C in the ex-vivo preparation, eCAPs were successfully elicited and presented a similar morphology to those seen in-vivo. However, there were discrepancies between the amplitude of eCAPs seen ex-vivo and in-vivo (see Fig. 3). For the experiment depicted in Fig. 3, eCAP amplitude reached ~200 μVpp at 37 °C ex-vivo, whereas it only reached ~80 μVpp in-vivo. This difference can be partially attributed to the distance between stimulation and recording sites, which was larger in-vivo given the recording cuff was implanted at the most proximal aspect of the ulnar nerve, and the stimulation cuff was implanted distal of the elbow. This is further corroborated in Table 1, where a substantial difference in eCAP width across all experiments can be seen when comparing average in-vivo values (0.17 ± 0.05 ms) to those ex-vivo at 37 °C (0.04 ± 0.02 ms). It is worth noting that a fixed cathodic stimulation pulse width of 100 μs was used throughout these experiments. A prior study on the recording of in-vivo eCAPs in pig ulnar nerves has highlighted that a pulse width of 500 μs is on the horizontal asymptotic section of the strength-duration curve, and that increasing this further had no effect on the excitation of fast fibres (Andreis et al., 2022a). However, the authors also note that fast fibres can still be recruited at a pulse width of 100 μs with higher stimulation currents, such as those used in this study (up to 16 mA, beyond the expected supramaximal level).

Given the ability to control temperature via a water bath in the ex-vivo system, properties in time and velocity domain plots were examined at temperatures ranging between 20 and 37 °C. In the time domain, this resulted in a decrease in eCAP duration and amplitude at temperatures closer to 37 °C, as shown in Fig. 4(a). Although we are unaware of directly comparable prior studies studying the effect of temperature on explanted large animal nerves ex-vivo, studies have been carried out on individual neurons and human nerves. In single-axon studies (Hodgkin and Katz, 1949; Rutkove, 2001), a slower depolarisation of sodium channels at decreased temperature resulted in a decreased CV. Slower depolarisation and repolarisation were also seen, producing a longer duration AP. Given the increased channel-open time at lower temperatures, larger depolarisation also occurred, producing an increase in AP amplitude. Bolton et al. (1981) have observed a similar effect to that seen in our study in experiments on in-vivo human median and radial nerves, where cutaneous temperature was varied between approximately 20 and 32 °C, which resulted in a decrease in both CAP amplitude and duration as temperature increased. Ludin and Beyeler (1977) conducted similar experiments on the median nerve at the wrist and elbow, and found the same trend at temperatures ranging between 26 and 36 °C. In addition, they also saw an increase in CAP amplitude between 22 and 26 °C. It is hypothesised that the decrease in eCAP duration seen in this study ex-vivo occurs as a result of an increased proportion of fast, myelinated fibres being activated at near-nerve temperatures approaching 37 °C, whereas the decrease in amplitude might be as a result of not only heating the nerve but potentially from doing so without oxygenation or refreshing the medium.

In the velocity domain, the MSE between average in-vivo and ex-vivo IVS plots decreased as the ex-vivo temperature approached that seen in-vivo (see Fig. 6). However, it is worth noting that modal ex-vivo eCAP CV tended to peak around 45 $m\,s^{-1}$ at 37 °C, whereas those in-vivo reached on average 60 $m\,s^{-1}$. We hypothesise that this small discrepancy in CV at 37 °C could be partly due to nerve deterioration, particularly in terms of myelinated fibres, after reheating the nerve in the ex-vivo system. In the velocity domain, it was also observed that increasing temperatures shift the resulting IVS plot to the right, implying that as the temperature approaches that seen in-vivo (37 °C), so does the modal eCAP CV (see Fig. 7(b)). This relationship between CV and temperature has been previously investigated in individual neurons and cat peripheral nerves, and was attributed predominantly to changes in sodium and potassium channel activity (Hodgkin and Katz, 1949; Douglas and Malcolm, 1955; Frankenhaeuser and Moore, 1963). These studies report that the CV will be slower at lower temperatures owing to the slower onset of sodium channel depolarisation. When comparing ex-vivo IVS data at 37 °C to that in-vivo at around the same temperature and for the same nerve, a clear correspondence can once again be seen, quantified using MSE as shown in Fig. 7(c).

Since there were no recordings conducted at 37 °C immediately after the nerve was explanted (i.e. the nerve was first chilled to 4 °C, then reheated gradually), we hypothesised that the change in amplitude can be partially attributed to the time elapsed since explanting the nerve without providing oxygenation, whilst simultaneously increasing its metabolic rate with increasing temperatures (Ohe et al., 2006; Gilglioni et al., 2018). Microscopic changes in the electrical coupling between the nerve and electrode ex-vivo could also affect the amplitude over time (Rocha et al., 2016; Spira and Hai, 2013). Given the interplay between temperature and time since explanting the nerve, a multivariate linear regression model was devised to investigate these two effects, which showed that the time since explanting the nerve and temperature

were negatively correlated with eCAP amplitude, but this change was not statistically significant for the data obtained (see Table 3).

Similarly to amplitude in the time domain, temperature and time since explantation can also impact modal eCAP CV in the velocity domain. A regression model was therefore fit with modal eCAP CV as the dependent variable, highlighting that time since explantation is negatively correlated with modal eCAP CV, and temperature is positively correlated. Following this model, modal eCAP CV decreases by $0.13\,m\,s^{-1}\,min^{-1}$, implying that over 5 h this would result in a decrease of around $39\,m\,s^{-1}$. This is larger than the decrease seen on average when comparing ex-vivo and in-vivo data at 37 to 38 °C (see Fig. 6(e)), but it is worth noting the positive correlation with temperature in this case. Regarding the impact of temperature, the quantified change in CV per degree centigrade was $2.17\,m\,s^{-1}\,°C^{-1}$. The effect of temperature on peripheral nerves has been previously examined predominantly from the perspective of motor and sensory fibres. One prior study has found that the CV of motor fibres of healthy ulnar nerves in the forearm decreased by $2.4\,m\,s^{-1}\,°C^{-1}$ for near-nerve temperatures ranging between 29 and 38 °C (Henricksen, 1956), which is in line with the results presented for this work. Another study on the sciatic nerve has found this factor to be instead 1.7–1.9 $m\,s^{-1}\,°C^{-1}$ (Gassel and Trojaborg, 1964), and studies focusing on surface rather than near-nerve temperature have found this to vary between 1.5–2.1 $m\,s^{-1}\,°C^{-1}$ (Rutkove, 2001; Halar et al., 1983), which is also similar to the factor obtained in this study. In summary, these regression results support our hypotheses H1, H2, and H4, but reject hypothesis H3. Specifically, both temperature and time post-explantation significantly impact eCAP modal CV, but this impact is not statistically significant on eCAP amplitude. Partial plots and histograms of residuals for the amplitude and modal CV linear regression models have been included as supplementary material, which further supports the applicability of linear regression for modelling modal CV but not amplitude.

The ex-vivo system and study have some limitations. First, the ex-vivo system itself could be further optimised and improved. In particular, the absence of oxygenation and not optimising the perfusion physiological saline medium will likely have impacted the viability of the nerve, and restricted the available experiment time after explantation. There was also a lag between setting the temperature on the water bath and this propagating throughout the water jacket, meaning very fine temperature steps were impractical to obtain. Given the need to transport the nerve between facilities, the initial ex-vivo temperature was always ~20 °C in this study. It would also be useful to investigate nerve activity in a setting where the nerve can be explanted and immediately transferred to an ex-vivo system at 37 to 38 °C, to confirm any effects arising from cooling and trends in time since explantation. Second, eCAP amplitude was used as a proxy for overall nerve viability or health in hypothesis H3, but there may be other measures to quantify this more clearly. In fact, the eCAP amplitude as detected by cuff electrodes can also be affected by other factors, such as the contact impedance between the nerve and electrodes. Third, this study focussed predominantly on results from electrical neuromodulation experiments. Although this offers valuable insights by examining eCAPs both in the time and velocity domain, these measurements are taken from the outside of the nerve, and hence consist of responses from large groups of individual fibres, both myelinated and unmyelinated (Andreis et al., 2022a). Nerve conduction studies have also been carried out in carpal tunnel syndrome (CTS) patients, where there is a reduction in median nerve myelination owing to compression of the nerve. Prior research showed thickly myelinated fibres are more sensitive to temperature compared to thinly myelinated fibres, as evidenced by CTS studies which resulted in sensory CV changes of 0.1–0.7 $m\,s^{-1}\,°C^{-1}$ instead (Rutkove, 2001; Wang et al., 1999; Ashworth et al., 1998). Therefore, individual fibre activity and characteristics could be investigated further in future, both in terms of electrical activity but also with histological analysis. Addressing the limitations mentioned above would significantly improve the confidence and utility of using ex-vivo systems for neuromodulation experiments.

5. Conclusions

This paper proposes a new approach for the development and assessment of an ex-vivo system for conducting neuromodulation experiments on large animal peripheral nerves. This would complement existing simulations and in-vivo experiments in neural interface development. Crucially, to the best of our knowledge, this is the first study to collect and compare recordings obtained from neuromodulation experiments on explanted nerves to those seen in-vivo, and to examine ex-vivo large animal nerve viability over time and at different temperatures.

The proposed ex-vivo system was capable of sustaining explanted peripheral nerves for several hours for neuromodulation experiments. At present, in-vivo experiments allowed for approximately 8 h of effective experimentation time. After explanting the nerve and allowing 1 to 2 h for transport, the ex-vivo system then allows for an additional 2 to 3 h of effective experimentation time. The experiments conducted followed a realistic use case of having to transport the nerve and were compared with in-vivo data for the first time. Such a system is important for complementing in-vivo experiments, by maximising the utility and potential experimental data to be collected from single or multiple nerves in a cost-effective and straightforward manner. This system could therefore be used for a range of research activities in neural interface development, such as the optimisation of materials, electrode or interface designs, and selecting and trialling new equipment, among others. The ability to capture additional experimental data following in-vivo experiments would also be vital for training ML models, which are becoming increasingly prevalent in biomedical engineering but require substantial and diverse datasets to produce accurate results.

Funding

M. Ribeiro was funded by UKRI grant EP/S023437/1.

CRediT authorship contribution statement

Mafalda Ribeiro: Writing – original draft, Software, Investigation, Formal analysis, Data curation, Conceptualization. **Felipe R. Andreis:** Writing – review & editing, Resources, Investigation, Data curation. **Leen Jabban:** Writing – review & editing, Investigation, Data curation. **Thomas G.N.dS. Nielsen:** Writing – review & editing, Resources, Project administration, Methodology, Investigation, Conceptualization. **Sergey V. Smirnov:** Writing – review & editing, Methodology, Conceptualization. **Christof Lutteroth:** Writing – review & editing, Supervision, Software. **Michael J. Proulx:** Writing – review & editing, Supervision, Software. **Paulo R.F. Rocha:** Writing – review & editing, Supervision, Conceptualization. **Benjamin Metcalfe:** Writing – review & editing, Supervision, Resources, Project administration, Funding acquisition, Conceptualization.

Declaration of competing interest

The authors declare that they have no known competing financial interests or personal relationships that could have appeared to influence the work reported in this paper.

Data availability

Data will be made available on request.

Appendix A. Supplementary data

Supplementary material related to this article can be found online at https://doi.org/10.1016/j.jneumeth.2024.110116.

References

Andreis, F.R., Metcalfe, B., Janjua, T.A.M., Fazan, V.P.S., Jensen, W., Meijs, S., Nielsen, T.G.N.d.S., 2024. Morphology and morphometry of the ulnar nerve in the forelimb of pigs. Anat. Histol. Embryol. 53 (1), e12972. http://dx.doi.org/10.1111/ahe.12972, arXiv:https://onlinelibrary.wiley.com/doi/pdf/10.1111/ahe.12972. e12972 AHE-02-23-OA-053.R1.

Andreis, F.R., Metcalfe, B., Janjua, T.A.M., Jensen, W., Meijs, S., dos Santos Nielsen, T.G.N., 2022a. The use of the velocity selective recording technique to reveal the excitation properties of the ulnar nerve in pigs. Sensors 22, http://dx.doi.org/10.3390/s22010058.

Andreis, F.R., Metcalfe, B., Janjua, T.A.M., Meijs, S., Favretto, M.A., Jensen, W., Nielsen, T.G.N.D.S., 2022b. A comparison of delay-and-add and maximum likelihood estimation for velocity-selective recording using multi-electrode cuffs. In: Proceedings of the Annual International Conference of the IEEE Engineering in Medicine and Biology Society. EMBS, Vol. 2022-July, pp. 4127–4130. http://dx.doi.org/10.1109/EMBC48229.2022.9870897.

Ashworth, N.L., Marshall, S.C., Satkunam, L.E., 1998. The effect of temperature on nerve conduction parameters in carpal tunnel syndrome. Muscle Nerve 21, 1089–1091. http://dx.doi.org/10.1002/(SICI)1097-4598(199808)21:8<1089::AID-MUS18>3.0.CO;2-P.

Bastian, C., Brunet, S., Baltan, S., 2020. Ex Vivo Studies of Optic Nerve Axon Electrophysiology. Springer US, New York, NY, pp. 169–177. http://dx.doi.org/10.1007/978-1-0716-0585-1_13.

Bliese, P., 2022. Multilevel modeling in R (2.7) a brief introduction to r, the multilevel package and the nlme package.

Bolton, C.F., Sawa, G.M., Carter, K., 1981. The effects of temperature on human compound action potentials. J. Neurol. Neurosurg. Psychiatry 44, 407–413. http://dx.doi.org/10.1136/jnnp.44.5.407.

Bottomley, J.M., LeReun, C., Diamantopoulos, A., Mitchell, S., Gaynes, B.N., 2020. Vagus nerve stimulation (VNS) therapy in patients with treatment resistant depression: A systematic review and meta-analysis. Compr. Psychiatry 98, 152156. http://dx.doi.org/10.1016/j.comppsych.2019.152156.

Cracchiolo, M., Ottaviani, M.M., Panarese, A., Strauss, I., Vallone, F., Mazzoni, A., Micera, S., 2021. Bioelectronic medicine for the autonomic nervous system: clinical applications and perspectives. J. Neural Eng. 18, http://dx.doi.org/10.1088/1741-2552/abe6b9.

Creasey, G.H., Ho, C.H., Triolo, R.J., Gater, D.R., DiMarco, A.F., Bogie, K.M., Keith, M.W., 2004. Clinical applications of electrical stimulation after spinal cord injury. J. Spinal Cord Med. 27, 365–375. http://dx.doi.org/10.1080/10790268.2004.11753774.

Douglas, W.W., Malcolm, J.L., 1955. The effect of localized cooling on conduction in cat nerves. J. Physiol. 130, 53–71. http://dx.doi.org/10.1113/jphysiol.1955.sp005392.

Ferrari, G.M.D., Stolen, C., Tuinenburg, A.E., Wright, D.J., Brugada, J., Butter, C., Klein, H., Neuzil, P., Botman, C., Castel, M.A., D'Onofrio, A., de Borst, G.J., Solomon, S., Stein, K.M., Schubert, B., Stalsberg, K., Wold, N., Ruble, S., Zannad, F., 2017. Long-term vagal stimulation for heart failure: Eighteen month results from the neural cardiac TherApy for heart failure (NECTAR-HF) trial. Int. J. Cardiol. 244, 229–234. http://dx.doi.org/10.1016/j.ijcard.2017.06.036.

Frankenhaeuser, B., Moore, L.E., 1963. The effect of temperature on the sodium and potassium permeability changes in myelinated nerve fibres of Xenopus laevis. J. Physiol. 169, 431–437. http://dx.doi.org/10.1113/jphysiol.1963.sp007269.

Fuglsang-Frederiksen, A., Pugdahl, K., 2011. Current status on electrodiagnostic standards and guidelines in neuromuscular disorders. Clin. Neurophysiol. 122, 440–455. http://dx.doi.org/10.1016/j.clinph.2010.06.025.

Gassel, M.M., Trojaborg, W., 1964. Clinical and electrophysiological study of the pattern of conduction times in the distribution of the sciatic nerve. J. Neurol. Neurosurg. Psychiatry 27, 351.

Gilglioni, E.H., Chang, J.-C., Duijst, S., Go, S., Adam, A.A.A., Hoekstra, R., Verhoeven, A.J., Ishii-Iwamoto, E.L., Elferink, R.P.J.O., 2018. Improved oxygenation dramatically alters metabolism and gene expression in cultured primary mouse hepatocytes. Hepatol. Commun. 2, 299–312. http://dx.doi.org/10.1002/hep4.1140/full.

Gribi, S., du Bois de Dunilac, S., Ghezzi, D., Lacour, S.P., 2018. A microfabricated nerve-on-a-chip platform for rapid assessment of neural conduction in explanted peripheral nerve fibers. Nature Commun. 9, 1–10. http://dx.doi.org/10.1038/s41467-018-06895-7.

Halar, E.M., DeLisa, J.A., Soine, T.L., 1983. Nerve conduction studies in upper extremities: skin temperature corrections. Arch. Phys. Med. Rehabil. 64, 412—416.

Harreby, K.R., Sevcencu, C., Jensen, W., 2013. In vitro large polyfascicular nerve model for assessment of fascicular recruitment characteristics of peripheral nerve interfaces. In: Converging Clinical and Engineering Research on Neurorehabilitation. Vol. 1, pp. 403–407. http://dx.doi.org/10.1007/978-3-642-34546-3_65.

Haugland, M., 1996. Flexible method for fabrication of nerve cuff electrodes. In: Annual International Conference of the IEEE Engineering in Medicine and Biology - Proceedings. pp. 359–360. http://dx.doi.org/10.1109/iembs.1996.656992.

Henricksen, J.D., 1956. Conduction Velocity of Motor Nerves in Normal Subjects and in Patients with Neurological Disorders (Ph.D. thesis). University of Minnesota.

Hodgkin, A.L., Katz, B., 1949. The effect of temperature on the electrical activity of the giant axon of the squid. J. Physiol. 109 (1–2), 240–249.

Johnson, E.W., Olsen, K.J., 1960. Clinical value of motor nerve conduction velocity determination. JAMA 172, 2030–2035. http://dx.doi.org/10.1001/jama.1960.03020180040007.

Koh, R.G., Zariffa, J., Jabban, L., Yen, S.C., Donaldson, N., Metcalfe, B.W., 2022. Tutorial: A guide to techniques for analysing recordings from the peripheral nervous system. J. Neural Eng. 19, http://dx.doi.org/10.1088/1741-2552/ac7d74.

Kuba, R., Brázdil, M., Kalina, M., Procházka, T., Hovorka, J., Nežádal, T., Hadač, J., Brožová, K., Sebroňová, V., Komárek, V., Marusič, P., Ošlejšková, H., Zárubová, J., Rektor, I., 2009. Vagus nerve stimulation: Longitudinal follow-up of patients treated for 5 years. Seizure 18, 269–274. http://dx.doi.org/10.1016/j.seizure.2008.10.012.

Li, J., Shi, R., 2006. A device for the electrophysiological recording of peripheral nerves in response to stretch. J. Neurosci. Methods 154, 102–108. http://dx.doi.org/10.1016/j.jneumeth.2005.12.007.

Ludin, H.P., Beyeler, F., 1977. Temperature dependence of normal sensory nerve action potentials. J. Neurol. 216, 173–180. http://dx.doi.org/10.1007/BF00313618.

Metcalfe, B.W., Hunter, A.J., Graham-harper-cater, J.E., Taylor, J.T., 2021. Array processing of neural signals recorded from the peripheral nervous system for the classification of action potentials. J. Neurosci. Methods 347, 108967. http://dx.doi.org/10.1016/j.jneumeth.2020.108967.

Nicolai, E.N., Settell, M.L., Knudsen, B.E., McConico, A.L., Gosink, B.A., Trevathan, J.K., Baumgart, I.W., Ross, E.K., Pelot, N.A., Grill, W.M., Gustafson, K.J., Shoffstall, A.J., Williams, J.C., Ludwig, K.A., 2020. Sources of off-target effects of vagus nerve stimulation using the helical clinical lead in domestic pigs. J. Neural Eng. 17, http://dx.doi.org/10.1088/1741-2552/ab9db8.

Ohe, C.G.V.D., Darian-Smith, C., Garner, C.C., Heller, H.C., 2006. Ubiquitous and temperature-dependent neural plasticity in hibernators. J. Neurosci. 26, 10590–10598. http://dx.doi.org/10.1523/JNEUROSCI.2874-06.2006.

Pérez-Carbonell, L., Faulkner, H., Higgins, S., Koutroumanidis, M., Leschziner, G., 2020. Vagus nerve stimulation for drug-resistant epilepsy. Pract. Neurol. 20, 189–198. http://dx.doi.org/10.1136/practneurol-2019-002210.

Prescott, M.J., Lidster, K., 2017. Improving quality of science through better animal welfare: the NC3Rs strategy. Lab Anim. 46 (4), 152–156. http://dx.doi.org/10.1038/laban.1217.

Ribeiro, M., Jabban, L., Andreis, F.R., dos Santos Nielsen, T.G.N., Rocha, P.R.F., Metcalfe, B., 2022. An in-vitro system for closed loop neuromodulation of peripheral nerves. In: 44th Annual International Conference of the IEEE in Medicine and Biology Conference. IEEE, Glasgow, pp. 2361–2364.

Ribeiro, M., Koh, R.G., Donnelly, T., Lutteroth, C., Proulx, M.J., Rocha, P.R., Metcalfe, B., 2023. Denoising and decoding spontaneous vagus nerve recordings with machine learning. In: 2023 45th Annual International Conference of the IEEE Engineering in Medicine & Biology Society. EMBC, Institute of Electrical and Electronics Engineers Inc., pp. 1–4. http://dx.doi.org/10.1109/EMBC40787.2023.10340443.

Rocha, P.R., Schlett, P., Kintzel, U., Mailänder, V., Vandamme, L.K., Zeck, G., Gomes, H.L., Biscarini, F., Leeuw, D.M.D., 2016. Electrochemical noise and impedance of au electrode/electrolyte interfaces enabling extracellular detection of glioma cell populations. Sci. Rep. 6, 1–10. http://dx.doi.org/10.1038/srep34843.

Rutkove, S.B., 2001. Effects of temperature on neuromuscular electrophysiology. Muscle Nerve 24, 867–882. http://dx.doi.org/10.1002/mus.1084.

Shin, U., Ding, C., Zhu, B., Vyza, Y., Trouillet, A., Revol, E.C.M., Lacour, S.P., Shoaran, M., 2022. NeuralTree: A 256-channel 0.227-μJ/class versatile neural activity classification and closed-loop neuromodulation SoC. IEEE J. Solid-State Circuits 57 (11), 3243–3257. http://dx.doi.org/10.1109/JSSC.2022.3204508.

Spira, M.E., Hai, A., 2013. Multi-electrode array technologies for neuroscience and cardiology. Nature Nanotechnol. 8, 83–94. http://dx.doi.org/10.1038/nnano.2012.265.

Sun, S., Delgado, J., Behzadian, N., Yeomans, D., Anderson, T.A., 2020. Ex vivo whole nerve electrophysiology setup, action potential recording, and data analyses in a rodent model. Curr. Protoc. Neurosci. 93, 481–489. http://dx.doi.org/10.1002/cpns.99.

Sun, F.T., Morrell, M.J., 2014. Closed-loop neurostimulation: The clinical experience. Neurotherapeutics 11, 553–563. http://dx.doi.org/10.1007/s13311-014-0280-3.

Tan, D.W., Schiefer, M.A., Keith, M.W., Anderson, J.R., Tyler, D.J., 2015. Stability and selectivity of a chronic, multi-contact cuff electrode for sensory stimulation in human amputees. J. Neural Eng. 12, http://dx.doi.org/10.1088/1741-2560/12/2/026002.

Tarotin, I., Mastitskaya, S., Ravagli, E., Perkins, J.D., Holder, D., Aristovich, K., 2022. Overcoming temporal dispersion for measurement of activity-related impedance changes in unmyelinated nerves. J. Neural Eng. 19, http://dx.doi.org/10.1088/1741-2552/ac669a.

Taylor, J., Schuettler, M., Clarke, C., Donaldson, N., 2012. The theory of velocity selective neural recording: A study based on simulation. Med. Biol. Eng. Comput. 50, 309–318. http://dx.doi.org/10.1007/s11517-012-0874-z.

Wang, A.K., Raynor, E.M., Blum, A.S., Rutkove, S.B., 1999. Heat sensitivity of sensory fibers in carpal tunnel syndrome. Muscle Nerve 22, 37–42. http://dx.doi.org/10.1002/(sici)1097-4598(199901)22:1<37::aid-mus7>3.0.co;2-g.

Waxman, S.G., 1980. Determinants of conduction velocity in myelinated nerve fibers. Muscle Nerve 3, 141–150. http://dx.doi.org/10.1002/mus.880030207.